

Fruit quality control by surface analysis using a bio-inspired soft tactile sensor

Pedro Ribeiro^{1,2,4}, Susana Cardoso^{1,2}, Alexandre Bernardino³ and Lorenzo Jamone⁴

Abstract—The growing consumer demand for large volumes of high quality fruit has generated an increasing need for automated fruit quality control during production. Optical methods have been proved successful in a few cases, but with limitations related to the variability of fruit colors and lighting conditions during tests. Tactile sensing provides a valuable alternative, although it comes with the need of a physical interaction that could damage the fruit. To overcome these limitations, we propose the usage of a recently developed soft tactile sensor for non-invasive fruit quality control. The ability of the sensor to detect very small forces and to finely analyze surfaces allows the collection of relevant information about the fruit by performing a very delicate physical interaction, that does not cause any damage. We report experiments in which such information is used to determine whether apples and strawberries are ripe or senescent. We test different configurations of the sensor and different classification algorithms, achieving very good accuracy for both apples (96%) and strawberries (83%).

I. INTRODUCTION

Fruit and vegetable consumption has steadily increased during the last two decades, having more than doubled since 1990 [1]. The larger production volumes required, together with a rising consumer demand for value and quality [2], have generated the need for a higher number of automated facilities [3]. In this context, the implementation of novel sensors and signal processing techniques to monitor food quality during the whole processing pipeline have gained traction recently [4].

Automatic fruit quality control is usually realized using either optical or tactile sensors. Optical technologies are the most developed and commonly used, as they are both non-invasive and easy to implement (often requiring only a camera). In what concerns the classification of fruits in regards to quality, various techniques have been presented in the past, reporting classification accuracy better than 90% for various parameters of interest in fruits and vegetables [5]. Although some industrial devices have been developed and are currently commercialized [6], automatic fruit control has not yet met widespread acceptance, as wide variability of defect types and fruit skin colour, in addition to changing lighting conditions, pose classification reliability issues [7].

In an effort to overcome the difficulties of optical detection, or to complement the optical detection information, tactile testing may provide useful data regarding the quality

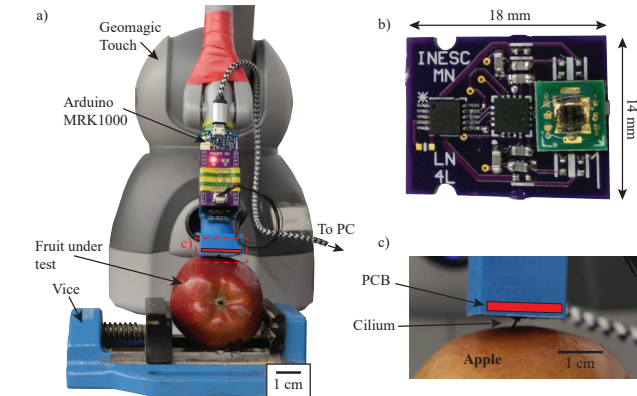


Fig. 1. a) Full experimental setup. b) Detail of the data acquisition PCB with mounted cilia. c) Single cilia scanning an apple surface. The red rectangle indicates where the data acquisition PCB is located.

of the fruit, especially in what concerns its internal condition. Two types of tactile measurements can be performed on fruits: palpation (determining the stiffness of the fruit) and textural analysis (determining the fruit surface topography).

The palpation technique has been the first developed and standardized type of tactile measurement, with the invention of the Magness-Taylor probe (a destructive measurement instrument) [8] and has since been used as the standardized method of measuring fruit quality through stiffness [9]. Non-destructive stiffness measurement devices and techniques have been developed in recent years, by lowering testing forces [10] and compacting testing devices [11]. In both these works a correlation between stiffness and quality is reported, but no attempt at quality classification is made. These types of sensors have also been integrated in robotic platforms, having reached a classification accuracy in distinguishing between ripe and green mangoes of 88% [12].

Although the surface characteristics of a fruit are generally accepted as a sensory factor in the perception of fruit quality, the quantification and analysis of this type of characteristics is still greatly underdeveloped [13]. The oldest reported tactile device used to measure this quantity on food products employed a tribometer to measure the coefficient of drag between the device and the surface of the food, thus providing an indirect measurement of the surface roughness [14]. The correlation between the age of peaches and their surface roughness, directly measured using atomic force microscopy, was reported in the same year [15]. Later, the usage of a tactile sensor to classify various fruit species given their textural characteristics was reported, achieving a

¹INESC - Microsystems and Nanotechnologies, Lisbon, Portugal

²Department of Physics, Instituto Superior Tecnico, University of Lisbon, Portugal

³Institute for Systems and Robotics, Lisbon, Portugal

⁴ARQ, School of Electronic Engineering and Computer Science, Queen Mary University of London, London, United Kingdom

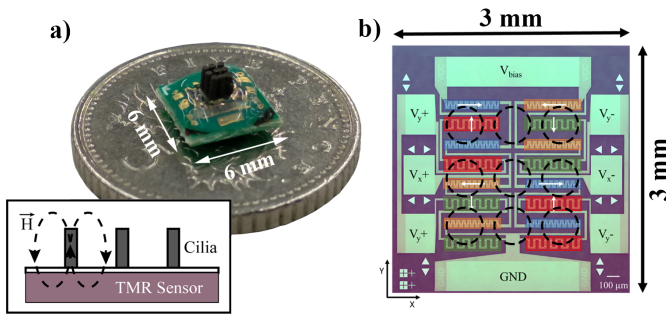


Fig. 2. a) Cilia sensor, with a 3x3 cilia matrix configuration. Inset: Schematic side view of the cilia sensor, with the magnetic field emitted by the cilia (\vec{H}). b) Microphotograph of the sensor die. The white arrows indicate the sensitive direction of each sensor region. Regions of the same colour have the same sensitive direction. The dashed circles show the cilia position on top of the sensor.

94% accuracy [16].

In this paper we demonstrate the use of a recently developed tactile sensor [17] for a fruit quality control task (Fig. 1). The sensor is inspired on the *ciliary* structure often found in living organisms: this structure consists of an elongated hair-like element known as *cilium* that is attached and protrudes out of a dendrite at its root, and is commonly found in insects and mammals allowing them to sense small forces and fluid flows [18]. Because of its geometry, our tactile sensor excels at measuring tangential forces and textures, and therefore it is a very good candidate for any application that can benefit from textural and surface topography information [17]. Moreover, because of the small size and extreme softness of the cilia, our sensor can detect very small forces, and therefore the exploration of the surface of the fruits can be done in a completely non-invasive way, i.e. without bringing any damage to the fruits. Therefore, the proposed method overcomes the limitations of optical systems (e.g. variability of fruit skin colour and effect of variable lighting conditions) without the need for an invasive exploration that could damage the fruit. Furthermore, due to its softness, this device is able to extract the fruit fine textural and hardness parameters simultaneously. The proposed detection method uses features extracted from the surface topography of a fruit and it applies machine learning techniques to classify fruits into ripe or senescent.

II. SENSOR DESCRIPTION

To measure the surface topography of the fruit, a bio-inspired cilia sensing element was used [19], and is shown in Fig. 2a). An array of magnetized elastic hairs is placed on top of a magnetic sensor. When these hairs bend, the magnetic signal over the sensor changes, and a monotonic relation between the cilia angle and the device signal is observed.

A. Magnetic cilia

The cilia in the sensor are composed of a mixture of 35% (in mass) polydimethylsiloxane (PDMS)¹ with 65% NdFeB

¹PDMS was prepared from Sylgard 184 at a mass proportion of 15 parts of elastomer to 1 part of curing agent

particles with an average diameter of 5 μm . The composite was shaped using a laser cut Poly(methylmethacrylate) mold (PMMA), into which the magnetic elastic composite was poured and left to cure for 90 minutes in an oven set at 70° C. After curing, to maximize the magnetic signal emitted by the composite, the moulded composite was further heated up to 100° C for 1 hour and 30 minutes under a magnetic field 1 T in the cilia axial direction. Finally, the composite (which is now moulded in cilia shape) is removed from mold and is then bonded to the magnetic sensor using an oxygen plasma bonding process. The produced cilia present a Young's modulus of approximately 1 MPa [20], resulting in an applied pressure of 3.5 kPa, much lower than cutting stresses for apples, which range from 200 kPa to 1 MPa [21].

B. Magnetic sensor

The underlying magnetic sensor (microfabricated at INESC-MN), is a 2D magnetic sensor based on the tunneling magnetoresistance (TMR) effect. A stack of metallic layers (with the structure, from top to bottom: [Ta 5/Ru 15]x3/Ni₈₀Fe₂₀ 4/Al₂O₃ 1.4/(Co₈₀Fe₂₀)₉₀B₁₀ 3/Ru 0.6/Ni₈₀Fe₂₀ 3/Mn₇₅Ir₂₅ 18/Ru 5/Ta 5, thicknesses in nm) was deposited and patterned into 640 sensing elements of 2x20 μm^2 area connected in series within a 3x3 mm² die (Fig. 2b).

To provide added robustness and easier signal conditioning [22] [23], the sensor was designed using a Wheatstone bridge architecture [24], which allows the measurements to be taken as a voltage differential centered around 0 V (in the ideal case) by combining TMR sensitive elements with anti-parallel sensitivities.

C. Electronic interface

An analog front-end was designed with the capability of eliminating the offset of the sensor and amplifying the corrected signal with a gain of up to 128 (V/V). This signal is then converted to a digital word by a 24-bit precision ADC unit at a 1 kSPS sampling rate, and the digital information is then transmitted to an Arduino MKR1000 through an I²C connection (and then relayed by the Arduino to the computer).

III. FRUIT QUALITY MEASUREMENT AND CLASSIFICATION

A. Setup

The number and geometry of the cilia placed on top of the sensor can be reconfigured, as different cilia geometries and configurations may perform better on specific types of fruits. Arrays of multiple cilia were found to present better detectivity when resolving unpatterned textured surfaces (since a larger number of cilia correspond to a higher magnetic material content and thus a stronger magnetic field), while single cilia devices can better resolve patterned features on a textured surface (due to a lower contact area with the sample) [19]. The following cilia configurations were tested:

- **Configuration A:** Single cilia with 400 μm diameter and 3 mm height.

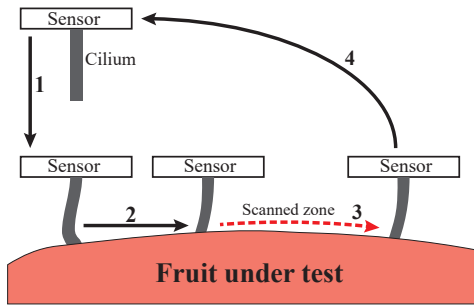


Fig. 3. Scanning sequence of the sensor. This sequence is repeated 10 times for each zone.

- **Configuration B:** Nine cilia in a 3x3 array over the sensor, each with 360 μm diameter and 1.6 mm height.
- **Configuration C:** Nine cilia in a 3x3 array over the sensor, each with 400 μm diameter and 3 mm height.

The sensing device is attached to a Geomagic Touch desktop haptic feedback interface, used as a desktop robotic arm in this work. Data acquisition and robot control was performed using a custom C# GUI based on the OpenHaptics libraries, running on a Windows 10 operating system.

B. Data acquisition and measurement procedure

The surface characteristics of a fruit are measured by scanning the sensor at a constant speed over its surface. However, as the sensor is facing the fruit under study upside down (as shown in Fig. 1c), care has to be taken when controlling the robotic arm, in order to avoid crushing the cilia against the sensor, which would produce an inaccurate surface topography measurement. The following measurement procedure was implemented (illustrated in Fig. 3):

- 1) Cilia is lowered against the surface of the fruit. When the derivative of the signal achieves a pre-determined threshold (meaning the cilia is bending upon contact with an obstacle), the arm stops its lowering movement.
- 2) The arm makes a fast short movement in one direction to tilt the cilia to a known direction (only to set the cilia tilting direction, but not its tilting angle).
- 3) The arm moves at a set speed of 1 mm/s, for a set distance (1 cm both types of fruit). The sensor signal and the arm position is recorded for the duration of this movement.
- 4) When the distance has been covered, the arm returns to its initial position and repeats the sequence from the beginning, for an arbitrary number of scans.

The robotic arm is controlled in open-loop for the whole duration of the measurement, except for step 1, where sensor data is used to detect when the cilia is touching the fruit surface.

Five adjustment scans (for which the data is not recorded) were done to ensure the cilia were in contact with the fruit for the whole scan duration, followed by 10 measurement scans over the same zone of the fruit.

Strawberries (Sabrina variety) and Apples (Braeburn variety) are among the most produced fruits in the United

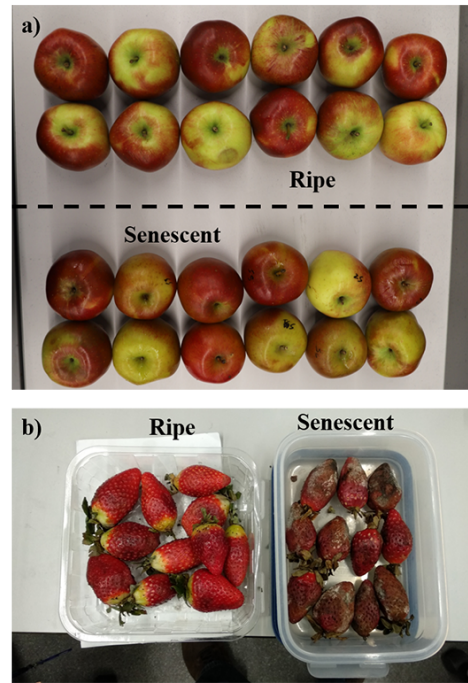


Fig. 4. Tested fruit pieces. a) Braeburn apples. b) Sabrina strawberries.

Kingdom [25] and were chosen to be tested (Fig. 4). For each type, a set of 12 ripe and 12 senescent fruits (performing a total of 24 fruits) were tested, with the scanning sequence being performed over two different sections of the same fruit (randomly chosen over the fruit equator). To ensure the fruit does not move during testing, a vice was used to gently clamp the piece of fruit (1a). Senescence in strawberries was achieved by natural processes, by keeping them for one week since the day of purchase at room temperature. As for apples, senescence was triggered by cold, placing fresh apples (at the day of purchase) in a freezer at -18°C for 24 hours, followed by a 24 hour thawing period at room temperature [26].

C. Features

As time passes, fruit starts becoming softer and more textured, as cells breakdown [27] and water is lost through evaporation [28].

For each scan of the analyzed fruit, a raw signal as shown in Fig. 5 is obtained, from which three features can be extracted:

- **Smoothness (S):** A moving average filter with a 1000 point moving window was applied to signal, and its derivative was then computed. The standard deviation of this derivative was taken as an estimation of smoothness (Fig. 5b).
- **Stiffness (E):** The average of the first 100 points of the measured signal were used as a metric of the fruit stiffness (Fig. 5a).
- **Texture (R):** A equiripple finite impulse response (FIR) high-pass filter with a cut-off frequency of 120 Hz was applied to the signal, with the standard deviation of the filtered signal being taken as a metric of the fruit texture

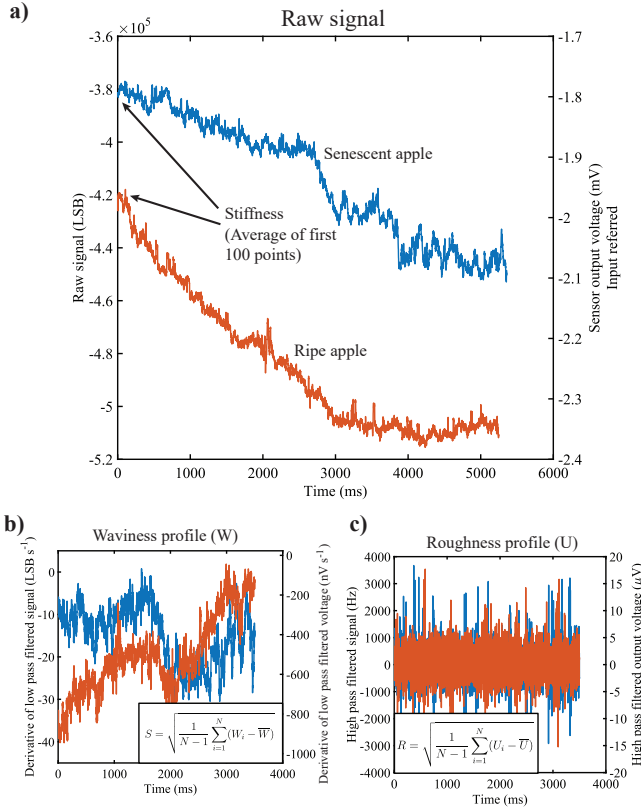


Fig. 5. Measured signal for an apple scan and derived values. a) Raw signal of the scan for a ripe and a senescent apple. b) Waviness profile, computed by low pass filtering and deriving the raw signal, used to determine the smoothness metric (inset). c) Roughness profile, computed by high pass filtering the raw signal, used to determine the texture metric (inset).

(Fig. 5c).

D. Classification algorithm

As the goal of this work is to classify fruit quality, and each fruit surface is scanned multiple times, a classifier capable of returning its decision margin of confidence is of interest, as it can be later plugged into a Bayesian update algorithm to achieve more accurate classification results. A data-driven approach was chosen, as the fruit surface correlation with quality is scarce in literature, and such an approach allows for the usage of the optimal thresholds for determining quality using the aforementioned parameters. Each classifier was trained independently for each type of fruit². For each type of fruit, two supervised classification algorithms were tested:

1) *Gaussian Naive Bayes classifier*: It was assumed that the measurements could be described by a trivariate Gaussian distribution,

$$P(S_i, E_i, R_i | F_k) \sim N(S_i, E_i, R_i | \mu_k, \Sigma_k), \quad (1)$$

where μ_k is the mean vector and Σ_k is the covariance matrix for the observations made of a certain type of fruit F_k , where k is the class of the fruit (ripe or senescent).

²I.e., the classifier trained for classifying the quality of apples was not used to classify strawberries and vice-versa

Therefore, as each passage of the sensor is made on the fruit, a new set of S_i, E_i, R_i features is obtained, and can be used to determine the probability of a fruit being of a certain class. As each passage is made on a fruit and a new set of metrics is obtained, the probability can be updated using

$$P(F_k | S_i, E_i, R_i) = P(F_k) \prod_i \frac{P(S_i, E_i, R_i | F_k)}{P(S_i, E_i, R_i)} \quad (2)$$

and a decision is made based on which class of fruit presents the highest probability.

2) *Random forest classifier*: The random forest classifier uses an ensemble of classification trees trained with the given data and expected responses for each data point. Each tree computes a prediction given a data point, and the class chosen by the greatest number of trees becomes the predicted class by the forest. Furthermore, the number of trees providing each verdict is known with the probability that the forest verdict is true being estimated by

$$P(F_k | S_i, E_i, R_i) = \frac{T_k}{T_T}, \quad (3)$$

where T_k is the number of trees in the forest supporting that a fruit belongs to a class k and T_T is the total number of trees. Given this probability, the joint probability of all the measurements belonging to a certain fruit k are then given by

$$P(F_k) = \prod_i P(F_k | S_i, E_i, R_i) \quad (4)$$

and the classification can be done by choosing the class presenting the highest probability. In this work, a Matlab R2018a implementation of this algorithm (TreeBagger class) was employed. A Forest of 100 trees was trained.

IV. RESULTS

All fruits were measured with the three different sensor configurations and classified with the methods presented in the previous section. Verification of the prediction was made using a leave-one-out cross-validation for each fruit. One of the two left out scans (chosen at random) was used for validation. This process was repeated for each of the fruits in the dataset. Outliers (usually caused by loss or poor contact between the cilia and the fruit during measurement) were removed by fitting all the measured data to a trivariate Gaussian distribution (using the 3 computed features) and eliminating all points that lied beyond a 95% interval of confidence (with one distribution fitted for each type and quality of fruit).

The methods were compared in what concerns effectiveness in classifying ripe and senescent fruits, and a study of the number of passages required to maximize the classification accuracy was also made.

A. Algorithm setup and performance assessment

Each testing set contains 10 scans (taking approximately 10 seconds per scan, for a total of 1 minute and 40 seconds of scan time per fruit) relative to the same zone of the

TABLE I
CLASSIFICATION PERFORMANCE USING THE THREE EXTRACTED FEATURES

Method	Fruit	Configuration A sensor			Configuration B sensor			Configuration C sensor		
		TP	TN	Accuracy	TP	TN	Accuracy	TP	TN	Accuracy
Gaussian Naive Bayes	Braeburn apple	11/12	12/12	0.96	10/12	11/12	0.88	9/12	8/12	0.71
Random Forest	Sabrina strawberry	7/12	10/12	0.71	10/12	7/12	0.71	10/12	10/12	0.83
Random Forest	Braeburn apple	10/12	12/12	0.92	10/12	11/12	0.88	9/12	11/12	0.83
Gaussian Naive Bayes	Sabrina strawberry	8/12	11/12	0.79	10/12	10/12	0.83	10/12	10/12	0.83

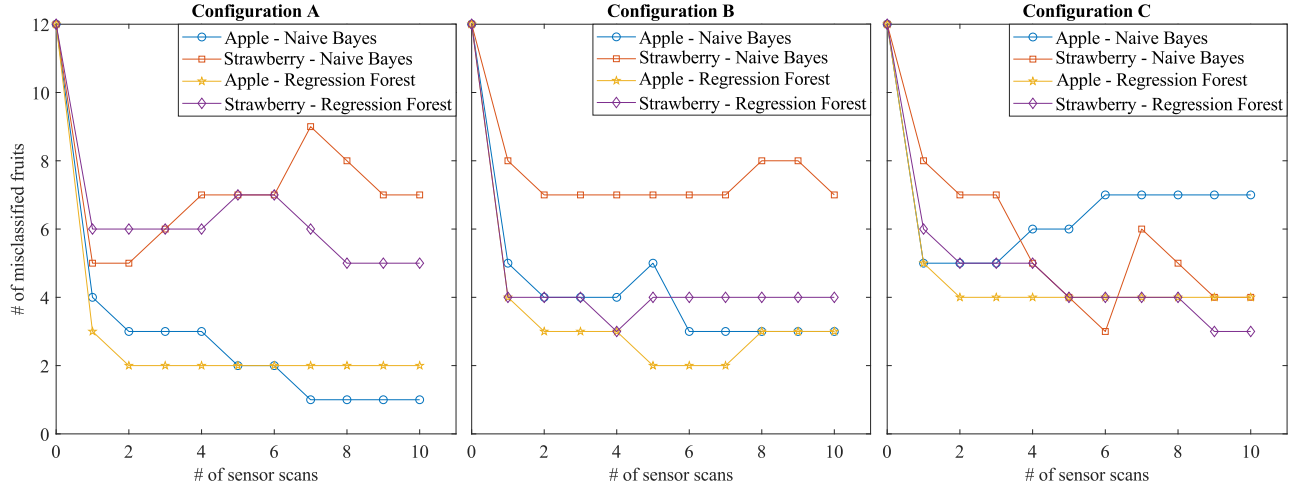


Fig. 6. Number of misclassified fruits for the three used sensor configurations as a function of the number of sensor scans over the fruit surface.

fruit, and all fruits were manually classified and labelled regarding their ripeness or senescence before starting the experiment. An equiprobability prior (50% probability for a ripe or senescent fruits being detected) was used for the Bayesian update. A fruit classified as ripe or senescent is considered a positive or negative occurrence respectively, and the classifier performance was rated in terms of its true positive and negative rates.

B. Classification performance

The classification performance was assessed in terms of the classification accuracy, which is presented alongside the true positive (TP) and true negative (TN) classifications in table I. The random forest algorithm was observed to have equivalent or marginally better performance than the Gaussian Naive Bayes algorithm.

The best overall performance was obtained for the apple tested using the sensor with configuration A cilia, with both algorithms providing accuracies above 90% (96% for the Gaussian Naive Bayes and 92% for the Random Forest algorithm). This is in contrast with the strawberry classification performance for this configuration, with an accuracy below 80%.

On the other hand, configuration B and C sensors performed better than configuration A in the classification for both employed algorithms, with a maximum accuracy of 83% being obtained when the random forest algorithm was used to classify strawberries with configuration B and C sensor data.

C. Bayesian update performance

The evolution of the classification error rate with the number of performed scans on the fruit was computed and is presented in figure 6.

For the most accurate classification cases (apples measured with configuration A cilia and strawberries measured with configuration C cilia), the number of misclassified fruits tends monotonically to lower values with an increasing number of scans when using the Random Forest algorithm. It is interesting to note that the progression of the error with the number of scans tends to oscillate instead of lowering monotonically when using the Naive Bayes algorithm, despite being of equivalent performance to the random forest in some cases (particularly for apples measured with configuration B sensor and strawberries measured with configuration C sensor), even when the end result of the classification is the same. This is indicative that the Random Forest algorithm should require less scans to achieve the best possible classification accuracy than the Naive Bayes algorithm.

The best performing combination (apples measured with configuration A sensor using Gaussian Naive Bayes algorithm) reached the minimum error in 7 scans, while the best performing Random Forest combination (apples measured with configuration A sensor) reached its minimum error in 3 scans. Thus, the number of required scans in a final device should be much lower than the 10 performed in our test, given that the right combination of cilia configuration is used for each fruit.

TABLE II

ACCURACY VS NUMBER OF FEATURES USED FOR CLASSIFICATION WITH GAUSSIAN NAIVE BAYES ALGORITHM

Sensor	Fruit	1 feature (E)	2 features ($E + R$)	3 features ($S + E + R$)
A	Apple	0.83	0.92	0.96
	Strawberry	0.63	0.79	0.71
B	Apple	0.71	0.88	0.88
	Strawberry	0.67	0.67	0.71
C	Apple	0.58	0.71	0.71
	Strawberry	0.63	0.83	0.83

D. Parameter influence on performance

The influence of the number of features used to train the classification algorithms on their performance was studied. The performance was evaluated using the data from the 10 measurements, with the same leave-one-out cross-validation method as described in subsection IV-A.

The accuracies obtained for the various sets of features is presented in tables II and III for the Gaussian Naive Bayes and Random Forest classification algorithms respectively. The stiffness parameter is used for the single parameter performance and the stiffness and texture parameter combination for the double parameter performance, as these provided the best classification performance in their respective categories.

For both algorithms, an improvement in classification performance is observed when two features are used in combination instead of a single parameter. However, when using the 3 features in combination, the performance improvement is either non-existent or marginal when compared with classification using two features. It is worth noticing that in some cases there is a loss in performance when using the 3 features.

V. DISCUSSION

The main defining difference between these configurations is the number of cilia on top of the sensor, with configuration A using a single cilia while B and C use a square matrix of 9 cilia. This is directly correlated with the area of contact of the sensor with the fruit under test and has a direct impact on the spatial resolution of the device, with devices using a lower number of cilia having been reported to have higher spatial resolution at the cost of providing a lower signal amplitude [19].

We hypothesize that this result comes from the difference between the surfaces of apples (which are smooth) and strawberries (which have bumps due to the seeds being present on the surface). When using a sensor with higher spatial resolution (as is the case with configuration A), any bumps on top of the surface under test will be accounted by the classification algorithm. While this is beneficial for a smooth fruit that starts acquiring bumps as it gets older, this is not the case fruits that are naturally bumpy. By using a higher contact surface, the result of the measurement will be averaged over the whole contact area, limiting the effect of existing bumps.

Therefore, the usage of a single cilia sensor should be used if the fruit is smooth, as it is capable of transducing

TABLE III

ACCURACY VS NUMBER OF FEATURES USED FOR CLASSIFICATION WITH RANDOM FOREST ALGORITHM

Sensor	Fruit	1 feature (E)	2 features ($E + R$)	3 features ($S + E + R$)
A	Apple	0.79	0.96	0.92
	Strawberry	0.63	0.79	0.79
B	Apple	0.75	0.88	0.88
	Strawberry	0.79	0.88	0.88
C	Apple	0.71	0.83	0.83
	Strawberry	0.63	0.83	0.83

the greatest amount of information possible about the fruit under test leading to the best possible performance. However, should the fruit have naturally occurring surface features, the usage of a cilia matrix is preferable even if at the cost of some performance, as the larger contact area will create an averaging effect of the surface texture, and with naturally occurring features averaged out there is no risk of these being learned by the classification algorithm.

It is also interesting to note that, in general, true negative detection is more accurate than true positive detection in this study, which could be advantageous in an industrial setting, as the lower chance of a senescent fruit being misclassified as ripe would maximize value to the final customer, while misclassified ripe fruits could be provided to a human operator for a more accurate quality assessment.

VI. CONCLUSION AND FUTURE WORK

This paper reports on the performance of a cilia tactile sensor in the quality control of apples and strawberries. Three sensors with different cilia configurations were used to test the fruits.

In general, across all the combinations of sensor/fruit tested, the random forest algorithm performed better than the Gaussian Naive Bayes, while reaching the maximum performance by requiring less fruit scans. Note that more sophisticated algorithms might lead to even better results: however, the goal of this work was not to compare algorithms, but to show that, regardless the specific algorithm, good results could be achieved by the sensor on this task, mainly because of the ability of the sensor to collect relevant data. Overall, assuming all three parameters are used in the classification algorithms, the best performing sensor for apple classification was configuration A device (96% accuracy), while for strawberries it was the configuration B device (83% accuracy). This is indicative that these type of sensors (configuration A) are better at classifying smooth surfaces; on the contrary, when classifying fruits with naturally occurring bumps on the surface (e.g. strawberries), it is preferable to use a sensor with a larger area of contact (configuration B), although with lower spatial resolution.

It was observed that the usage of more than one parameter brings a significant improvement in classification performance, but the usage of three parameters provides the best classification performance, despite being a marginal improvement over the 2 parameter case.

For future work, the magnetic sensor under the cilia will be improved to provide a 2D response, which would allow the computation of the cilia angle over the sensor, providing additional information on the fruit characteristics. Furthermore, given the high classification performance obtained, classification into more classes than binary will be tested, which could provide interesting information on how to maximize the value of a whole batch, e.g. a top-tier fruit would be sold fresh, but a low-tier (but not rotten) fruit could be processed into another food product.

ACKNOWLEDGEMENTS

We thank FabLab Lisboa for providing access and assistance with the laser cutting equipment. P. Ribeiro acknowledges FCT for his PhD grant SFRH/BD/130384/2017. S. Cardoso acknowledges FCT for grants NORTE-01-0145-FEDER-22090, MAGLINE-LISBOA-01-0247-FEDER-17865 and MagScopy4IHC-LISBOA-01-0145-FEDER-031200. A. Bernardino acknowledges FCT project UID/EEA/50009/2019 and European Commission project ORIENT (ERC/2016/693400). This work was partially supported by the EPSRC UK (with projects MAN3, EP/S00453X/1, and NCNR, EP/R02572X/1).

REFERENCES

- [1] Food and Agriculture Organization of the United Nations, "Global production of fresh fruit from 1990 to 2018 (in million metric tons)," 2018.
- [2] A. F. L. Camelo, *Manual for the Preparation And Sale of Fruits And Vegetables from Field to Market: Fao Agricultural Services Bulletin No. 151*. Food & Agriculture Organization of the United Nations, 2005.
- [3] Y. Edan, S. Han, and N. Kondo, *Automation in Agriculture*, pp. 1095–1128. Berlin, Heidelberg: Springer Berlin Heidelberg, 2009.
- [4] S. Wolfert, L. Ge, C. Verdouw, and M.-J. Bogaardt, "Big data in smart farming – a review," *Agricultural Systems*, vol. 153, pp. 69 – 80, 2017.
- [5] B. Zhang, B. Gu, G. Tian, J. Zhou, J. Huang, and Y. Xiong, "Challenges and solutions of optical-based nondestructive quality inspection for robotic fruit and vegetable grading systems: A technical review," *Trends in Food Science and Technology*, vol. 81, pp. 213 – 231, 2018.
- [6] V. Leemans and M.-F. Destain, "A real-time grading method of apples based on features extracted from defects," *Journal of Food Engineering*, vol. 61, no. 1, pp. 83 – 89, 2004. Applications of computer vision in the food industry.
- [7] D. Unay, B. Gosselin, O. Kleyne, V. Leemans, M.-F. Destain, and O. Debeir, "Automatic grading of bi-colored apples by multispectral machine vision," *Computers and Electronics in Agriculture*, vol. 75, no. 1, pp. 204 – 212, 2011.
- [8] J. R. Magness and G. F. Taylor, *An improved type of pressure tester for the determination of fruit maturity /,* vol. no.350. Washington, D.C. :U.S. Dept. of Agriculture., <https://www.biodiversitylibrary.org/bibliography/66090> — Cover title.
- [9] J. A. Abbott, "Quality measurement of fruits and vegetables," *Postharvest Biology and Technology*, vol. 15, pp. 207–225, mar 1999.
- [10] C. Ortiz, C. Blanes, and M. Mellado, "An ultra-low pressure pneumatic jamming impact device to non-destructively assess cherimoya firmness," *Biosystems Engineering*, vol. 180, pp. 161 – 167, 2019.
- [11] R. V. Aroca, R. B. Gomes, R. R. Dantas, A. G. Calbo, and L. M. G. Gonçalves, "A wearable mobile sensor platform to assist fruit grading," *Sensors*, vol. 13, no. 5, pp. 6109–6140, 2013.
- [12] L. Scimeca, P. Maiolino, D. Cardin-Catalan, A. P. d. Pobil, A. Morales, and F. Iida, "Non-destructive robotic assessment of mango ripeness via multi-point soft haptics," in *2019 International Conference on Robotics and Automation (ICRA)*, pp. 1821–1826, May 2019.
- [13] J. Chen, "Surface texture of foods: Perception and characterization," *Critical Reviews in Food Science and Nutrition*, vol. 47, no. 6, pp. 583–598, 2007. PMID: 17653982.
- [14] J. Chen, T. Moschakis, and P. Nelson, "Application of surface friction measurements for surface characterization of heat-set whey protein gels," *Journal of Texture Studies*, vol. 35, no. 5, pp. 493–510, 2004.
- [15] H. Yang, H. An, G. Feng, and Y. Li, "Visualization and quantitative roughness analysis of peach skin by atomic force microscopy under storage," *LWT - Food Science and Technology*, vol. 38, no. 6, pp. 571 – 577, 2005.
- [16] J. Zhou, Y. Meng, M. Wang, M. S. Memon, and X. Yang, "Surface roughness estimation by optimal tactile features for fruits and vegetables," *International Journal of Advanced Robotic Systems*, vol. 14, no. 4, p. 1729881417721866, 2017.
- [17] P. Ribeiro, M. A. Khan, A. Alfadhel, J. Kosel, F. Franco, S. Cardoso, A. Bernardino, A. Schmitz, J. Santos-Victor, and L. Jamone, "Bioinspired ciliary force sensor for robotic platforms," *IEEE Robotics and Automation Letters*, vol. 2, pp. 971–976, April 2017.
- [18] T. A. Keil, "Functional morphology of insect mechanoreceptors," *Microscopy Research and Technique*, vol. 39, no. 6, pp. 506–531, 1997.
- [19] P. Ribeiro, S. Cardoso, A. Bernardino, and L. Jamone, "Highly sensitive bio-inspired sensor for fine surface exploration and characterization," in *Submitted to 2020 IEEE/RSJ International Conference on Robotics and Automation*, IEEE, may 2020.
- [20] P. Ribeiro, M. A. Khan, A. Alfadhel, J. Kosel, F. Franco, S. Cardoso, A. Bernardino, J. Santos-Victor, and L. Jamone, "A miniaturized force sensor based on hair-like flexible magnetized cylinders deposited over a giant magnetoresistive sensor," *IEEE Transactions on Magnetics*, vol. 53, no. 11, pp. 1–5, 2017.
- [21] A. A. Khan and J. F. Vincent, "Compressive stiffness and fracture properties of apple and potato parenchyma," *Journal of texture studies*, vol. 24, no. 4, pp. 423–435, 1993.
- [22] J. S. Moreno, D. R. Muñoz, S. Cardoso, S. C. Berga, A. E. N. Antón, and P. J. P. de Freitas, "A non-invasive thermal drift compensation technique applied to a spin-valve magnetoresistive current sensor," *Sensors*, vol. 11, pp. 2447–2458, feb 2011.
- [23] Honeywell International Inc., "Handling sensor bridge offset." Application Note 212.
- [24] P. P. Freitas, S. Cardoso, R. Ferreira, V. C. Martins, A. Guedes, F. A. Cardoso, J. Loureiro, R. Macedo, R. C. Chaves, and J. Amaral, "Optimization and integration of magnetoresistive sensors," *SPIN*, vol. 01, pp. 71–91, jun 2011.
- [25] F. Faostat, "Statistical databases," *Food and Agriculture Organization of the United Nations*, 2018.
- [26] J. M. Lyons, "Chilling injury in plants," *Annual Review of Plant Physiology*, vol. 24, no. 1, pp. 445–466, 1973.
- [27] M. F. Barnes and B. J. Patchett, "Cell wall degrading enzymes and the softening of senescent strawberry fruit," *Journal of Food Science*, vol. 41, no. 6, pp. 1392–1395, 1976.
- [28] H. P. Gould, *Evaporation of apples*. No. 291-300, US Dept. of Agriculture, 1907.